Radiophysics and Quantum Electronics, Vol. 47, Nos. 5–6, 2004

WAVE THEORY OF A TRAVELING-WAVE TUBE OPERATED NEAR THE CUTOFF

A. P. Kuznetsov,[1] S. P. Kuznetsov,[1] A. G. Rozhnev,[2*]
E. V. Blokhina,[2] and L. V. Bulgakova[3]

UDC 621.385.6

We outline the main principles of the wave theory of interaction between an electron beam and waves in a slow-wave structure near the edge of the transmission band. Formulation of the basic equations and the boundary conditions is considered taking consistently into account that the interaction parameter is small. A comparison of the results with a discrete version of the theory is discussed. We also consider the starting conditions for the oscillation regime, the linear amplification regimes, and some effects found within the framework of the nonstationary nonlinear theory, e. g., parasitic self-excitation in the amplification regime and hard excitation of the oscillation regime.

1. INTRODUCTION

In the history of Saratov workshops on microwave electronics, one can distinguish several problems of particular importance, whose discussion always attracted considerable attention. Among such problems, we should mention the theory of a traveling-wave tube (TWT) with a chain of coupled cavities (coupled-cavity TWT) or, more generally, the theory of interaction between an electron beam and an electromagnetic field near the edge of the transmission band of a slow-wave system. This problem was intensely studied in the eighties. At the workshops, lectures discussing discrete interaction [1] and the theory of excitation of periodic structures [2, 3] were presented and the results of our studies in the wave theory of a TWT operated near the cutoff [4–14] were reported. The objective of the present paper is to generalize the results which we obtained and to clarify the physical picture of interaction between an electron beam and a field near the edge of the transmission band of a slow-wave system.

Our main task was to develop a theory describing the main physical effects observed during interaction between an electron beam and a field near the edge of the transmission band using the minimum set of dimensionless parameters. This theory should, in a certain sense, be a counterpart of the Pierce theory in this frequency region. The fundamental approach consists in development of a theory for exactly the processes near the cutoff and ensuring that this theory transforms to the Pierce theory for a fairly large detuning from the cutoff frequency.

A coupled-cavity TWT represents a sequence of coupled cavities through which an electron beam moves (Fig. 1*a*). Since the electrodynamic structure is periodic, its dispersion curve in the wavenumber–frequency diagram is also periodic and has a period $2\pi/d$. The dispersion curve of an electron beam with velocity v_0 is a straight line. It is clearly seen that, by varying the accelerating voltage V_0, it is possible to provide for beam–wave interaction in the middle of the transmission band, near the high-frequency cutoff,

* RozhnevAG@info.sgu.ru

[1] Saratov Branch of the Institute of Radioengineering and Electronics of the Russian Academy of Sciences; [2] N. G. Chernyshevsky Saratov State University; [3] Saratov State Academy of Law, Saratov, Russia. Translated from Izvestiya Vysshikh Uchebnykh Zavedenii, Radiofizika, Vol. 47, Nos. 5–6, pp. 399–418, May–June, 2004. Original article submitted June 25, 2004.

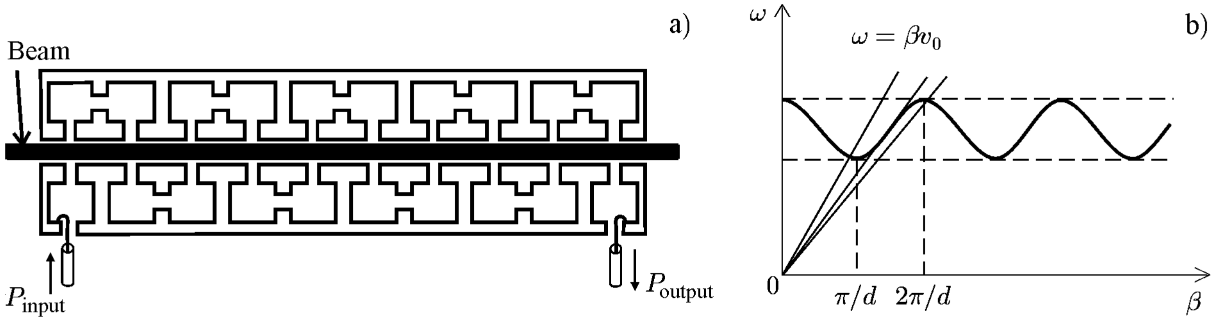

Fig. 1. Coupled-cavity TWT: sketch of the device (*a*) and the dispersion curve (*b*).

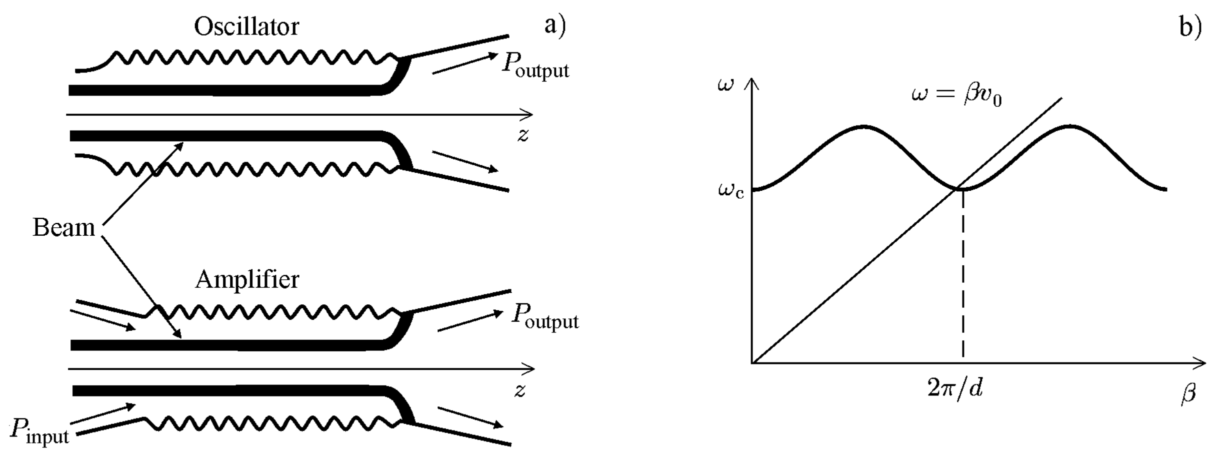

Fig. 2. Relativistic orotrons: the oscillator and amplifier (*a*) and the dispersion curve (*b*).

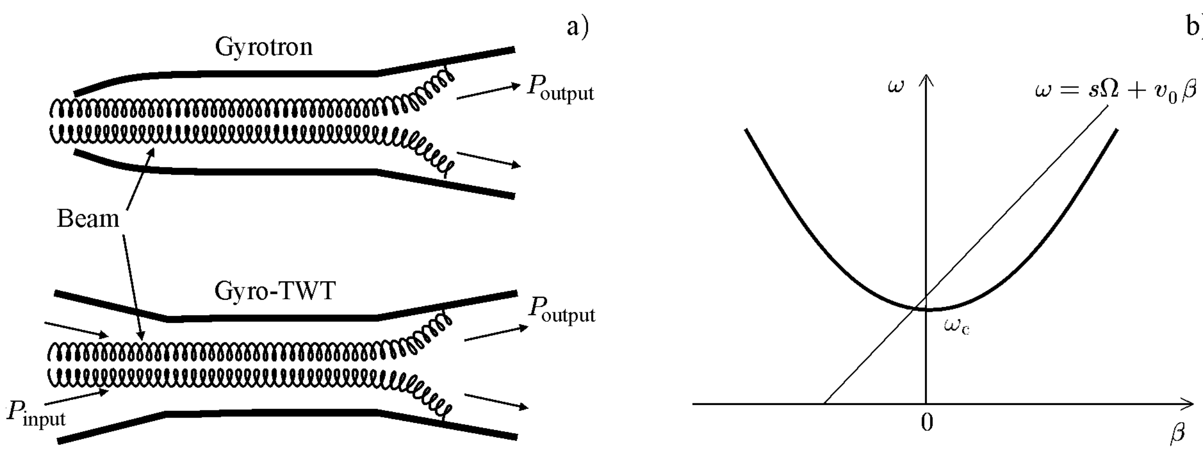

Fig. 3. Gyro-devices operated near the cutoff frequency of a smooth waveguide.

and near the low-frequency cutoff (Fig. 1*b*). The possibility of gradually passing from interaction with forward waves to interaction with backward waves by tuning the accelerating voltage is the most interesting feature of this system from the theoretical viewpoint.

It appears that the developed theory applies not only for a coupled-cavity TWT, but also for a broad range of electron devices. One of them is a relativistic orotron, which represents a corrugated waveguide in which a relativistic electron beam moves (Fig. 2*a*). The degree of corrugation is fairly weak, and, therefore, the dispersion curve of the system is obtained by periodically continuing the dispersion curve of a smooth waveguide.

Different spatial harmonics are coupled, forming the dispersion curve of a corrugated waveguide (Fig. 2*b*), near the wavenumbers $\beta = \pi\,(2n+1)/d$, where $n = 0, \pm 1, \ldots$. The beam–field synchronism is realized near the low-frequency cutoff where $\beta_0 \sim 2\pi/d$, and, hence, an orotron is called a 2π device. An orotron can be operated in both oscillation and amplification modes.

Notably, the same physical concept and the same equations of excitation describe the operation of devices in which the periodic structure is absent, but the interaction takes place, as in the previous case, near the cutoff frequency. A gyrotron is an example of such a device (Fig. 3*a*). Without going deep into the details, we only mention that with the variation in the magnetic field, the dispersion curve of an electron beam is shifted parallel to itself, and the interaction can occur both with forward or backward waves and in the immediate vicinity of the edge of the transmission band (Fig. 3*b*).

It is interesting to note that the stationary theory of a gyrotron with nonfixed field structure was proposed in 1973 [15], a long time before the papers discussed here appeared, while the nonstationary theory [16], somewhat later than the equations of the nonstationary theory of a coupled-cavity TWT were published [4].

2. BASIC EQUATIONS

As for any electron device, the theory of interaction near the edge of the transmission band comprises equations of excitation of a field and motion of electrons. The equations of motion are identical to the equations of the conventional theory of TWT. The main problems are related to the formulation of the equations of excitation. We will not make an historical review of various attempts to derive the equations of excitation near the cutoff and only mention that a considerable contribution to the solution of this problem was done by V. A. Solntsev and his disciples [17–21]. There are several methods of deriving these equations, and they all lead to the same result if only the time-dependent processes whose spectrum is located in the immediate vicinity of the edge of the transmission band are described. If a chain of relatively weakly coupled cavities is considered, then it seems most reasonable to use the equations of excitation of periodic structures as the basis for deriving these equations [22].

We represent the total electric field as a series of eigenfunctions with an additional term responsible for the space-charge field:

$$\mathbf{E}(x,y,z,t) = \sum_s \sum_n C_{sn}(t)\mathbf{E}_{0s}(x,y,z-nd) - \nabla\,\Phi(x,y,z). \tag{1}$$

Here, $C_{sn}(t)$ is the amplitude of the s-type oscillation localized near the nth cavity and $\mathbf{E}_s(x,y,z,t) = \Sigma_n C_{sn}(t)\mathbf{E}_{0s}(x,y,z-nd)$ is the field distribution of this type of oscillations. Since the cavities are assumed identical, the oscillations localized near the nth cavity are obtained by translation of oscillations of the "zeroth" cavity. It is important to mention that the boundary-value problem which permits one to calculate the eigenfunctions $\mathbf{E}_{ns} = \mathbf{E}_{0s}(x,y,z-nd)$ is formulated such that this eigenfunction is not localized in one cavity, but is also nonzero in other cavities. This makes it possible to take into account the "penetration" of the oscillation fields from the "own" cavity to the "neighboring" ones.

The following equations are valid for the coefficients C_{sn}:

$$\frac{\partial C_{sn}(t)}{\partial t} - i\sum_m \omega_{sm} C_{s\,(n-m)}(t) = -\int \mathbf{j}(x,y,z,t)\mathbf{E}^*_{0s}(x,y,z-nd)\,\mathrm{d}V. \tag{2}$$

Here, $\mathbf{j}(x,y,z,t)$ is the current density of the electron beam, the integration is performed over the entire waveguide volume, and ω_{sn} are the coefficients of expansion of the dispersion characteristic in a Fourier series:

$$\omega_s(\beta) = \sum_n \omega_{sn}\exp(in\beta d). \tag{3}$$

Equations (1)–(3) are rigorous and can, in principle, be used to develop the theory of a coupled-cavity TWT, but this will be a discrete version of the theory. Our goal is to obtain wave equations based on the fact that small parameters, associated with a narrow spectrum of wavenumbers and weak interaction, exist in this problem.

We make the usual assumption that an electron beam efficiently interacts with one electrodynamic-structure mode synchronous to it. Then we leave one term, corresponding to the synchronous field, in the sum over the index s in Eq. (1). Applying continuous Fourier transform over the longitudinal coordinate z to this field, we obtain

$$\mathbf{E}_s(x,y,t,\beta) = \mathbf{E}_{0s}(x,y,\beta)\sum_n C_{sn}(t)\exp(i\beta nd),$$

$$\mathbf{E}_{0s}(x,y,\beta) = \int\limits_{-\infty}^{+\infty} \mathbf{E}_{0\beta}(x,y,z)\exp(-i\beta z)\,\mathrm{d}z, \qquad \mathbf{j}(x,y,\beta,t) = \int\limits_{-\infty}^{+\infty} \mathbf{j}(x,y,z,t)\exp(-i\beta z)\,\mathrm{d}z. \tag{4}$$

Then we make the following assumptions:

— the spectral components of a signal are located near the cutoff wavenumber β_0;

— the transverse distribution of the field for wavenumbers in the region $|\beta - \beta_0| \ll \beta_0$ can be assumed independent of β;

— the nonsynchronous terms on the right-hand side of excitation equation (1) can be neglected.

With allowance for these approximations, we expand the dispersion relation at the extremum point in a Taylor series near the cutoff wavenumber and keep two main terms

$$\omega_s(\beta) = \omega_{0s} \mp \frac{|\omega_s''(\beta_0)|}{2}(\beta-\beta_0)^2, \qquad |\beta-\beta_0| \ll \beta_0, \tag{5}$$

where $\omega_{0s} = \omega_s(\beta_0)$ and the prime denotes the derivative with respect to the argument. Hereafter in all equations, the upper and lower signs correspond to the case of interaction near the high- and low-frequency cutoffs, respectively.

The second assumption permits one to represent the field of a cavity as the product of vector eigenfunctions and the field amplitude:

$$\mathbf{E}_{0s}(x,y,\beta) \approx E_{0s}(\beta_0)\boldsymbol{\psi}(x,y), \qquad \mathbf{E}_s(x,y,\beta,t) \approx E_s(\beta,t)\boldsymbol{\psi}(x,y), \tag{6}$$

where E_{0s} is the amplitude of the longitudinal component of the electric field of the mode, synchronous to the electron beam, on the system axis and $\boldsymbol{\psi}(x,y)$ is the vector eigenfunction normalized by the condition $\psi_z(0,0) = 1$. The excitation equation

$$\frac{\partial E_s(\beta,t)}{\partial t} - i\omega_s(\beta_0)E_s(\beta,t) \pm i\frac{|\omega_s''(\beta_0)|}{2}(\beta-\beta_0)^2\,E_s(\beta,t) = -|E_0(\beta_0)|^2\,I(\beta,t)$$

$$I(\beta,t) = \int\limits_{S_\perp} \mathbf{j}(x,y,\beta,t)\boldsymbol{\psi}^*(x,y)\,\mathrm{d}S, \tag{7}$$

is satisfied for $E_s(\beta,t)$ in the (β,t) representation. Here $I(\beta,t)$ is the excitation integral and $S_\perp$ is the cross section of the cavity.

To obtain equations in the spatio-temporal representation, one should introduce the slowly varying amplitudes $E(z,t) = \mathrm{Re}[\mathcal{E}(z,t)\exp[i\,(\omega_{0s}t - \beta_0 z)]]$ and $I(z,t) = \mathrm{Re}[J(z,t)\exp[i\,(\omega_{0s}t - \beta_0 z)]]$ of the field and the current, respectively, extract the components, corresponding to the wave with wavenumber β_0, from the total field, and perform inverse Fourier transform over the coordinate. As a result, we obtain the excitation equation of the slowly varying amplitude of the field (hereafter the subscript s is omitted for brevity):

$$\frac{\partial \mathcal{E}}{\partial t} \pm i\frac{|\omega''(\beta_0)|}{2}\frac{\partial^2 \mathcal{E}}{\partial z^2} = -\frac{|\omega''(\beta_0)|\,\beta_0^3}{2}RJ(z,t). \tag{8}$$

This equation describes the effect of the electron beam on the field. It is easy to understand that the equation takes into account only two spatial harmonics synchronous to the beam in the case where the dispersion characteristics of the electron beam and the slow-wave system are crossed in the vicinity of the extremum point. Equation (8) comprises a quantity R with impedance dimension, which we call the modified coupling impedance:

$$R = \frac{2\,|E_0(\beta_0)|^2}{|\omega''(\beta_0)|\,\beta_0^3}\,. \tag{9}$$

This quantity is constant and frequency-independent. Straightforward methods can be proposed to measure R, and it can be shown that the modified coupling impedance is expressed in terms of the conventional coupling impedance $R_\pm(\beta)$ of spatial harmonics by the formula

$$R = \lim_{\beta\to\beta_0} \frac{\beta-\beta_0}{\beta_0} R_\pm(\beta). \tag{10}$$

Excitation equation (8) is parabolic, and its appearance in the theory is directly related to the use of approximate expansion (5) for the dispersion relation of the synchronous mode. Obviously, the condition of applicability of this expansion relates the quantity $\Delta\omega = \max\,|\omega-\omega_0|$, defined over all frequency components of the signal amplified or generated in the system (the quantity $\Delta\omega$ specifies the localization of the Fourier spectrum near the cutoff frequency) and the total observation time T. The form of this relationship depends on the particular type of the dispersion relation. For example, the condition $\omega'''(\beta_0) = 0$ is satisfied in many cases for symmetry reasons. The validity conditions for the parabolic equation are given by two inequalities

$$\Delta\omega \ll |\omega''(\beta_0)|^2/|\omega^{\mathrm{IV}}(\beta_0)|, \qquad (\Delta\omega)^2\,T \le |\omega''(\beta_0)|^2/|\omega^{\mathrm{IV}}(\beta_0)|.$$

As was mentioned above, the equations of motion remain the same as for the conventional theory of TWT. If the electron phase is introduced as $\theta = \omega_0 t - \beta_0 z$, then the equation of motion is written in terms of Lagrange variables as

$$\frac{\mathrm{d}\theta}{\mathrm{d}z} = \frac{\omega_0}{v_z} - \beta_0, \tag{11}$$

$$\frac{\mathrm{d}\mathbf{r}}{\mathrm{d}z} = \frac{\mathbf{p}}{p_z}, \qquad \frac{\mathrm{d}\mathbf{p}}{\mathrm{d}z} = -\frac{e}{v_z}\left(\mathbf{E} + [\mathbf{v},\mathbf{B}]\right), \tag{12}$$

where $\mathbf{p} = m_0\gamma\mathbf{v}$ is the momentum, γ is the Lorentz factor, and m_0 is the electron rest mass.

Since our goal is to develop a very simple theory which could adequately describe the features of interaction near the cutoff, we adopt the following conventional approximations:

(i) the damping in this system at this stage is neglected;

(ii) the variation in the electron energy is assumed small;

(iii) the electron beam is assumed nonrelativistic;

(iv) the space-charge effects can be neglected;

(v) an unbounded focusing magnetic field is present.

Any of approximations (i)–(iv) can easily be rejected, if necessary, within the framework of the one-dimensional theory. Taking into account the bounded focusing magnetic field requires consideration of three-dimensional motion of electrons, which is possible, in principle, but significantly complicates numerical simulation and is therefore not considered here.

Introducing dimensionless variables and parameters, which are discussed later, we arrive at the system of equations describing the nonstationary processes near the cutoff frequency of a periodic slow-wave structure

$$\frac{\partial F}{\partial\tau} \pm i\,\frac{\partial^2 F}{\partial\xi^2} = iI, \qquad I = \frac{1}{\pi}\int_0^{2\pi} \exp(-i\theta)\,\mathrm{d}\theta_0, \tag{13}$$

TABLE 1.

$\tau = \lvert\omega''(\beta_0)\rvert\,\beta_0^2 t\varepsilon/2$	Normalized time
$\xi = \varepsilon\beta_0 z$	Normalized coordinate
$F = \mathcal{E}/(\beta_0 V_0 \varepsilon^2)$	Slowly varying amplitude of the field
$I = J/I_0$	Slowly varying amplitude of the currrent
$l = \varepsilon\beta_0 L$	Dimensionless length of the system
$Bl = (\beta_0 - \omega_0/v_0)\,L$	Relative angle of transit of the electron beam and the field at the cutoff frequency
$\Omega l^2 = 2\,(\omega - \omega_0)\,L^2/\lvert\omega''(\beta_0)\rvert$	Frequency detuning from cutoff
$\varepsilon^4 = I_0 R/(2V_0)$	Interaction parameter

$$\frac{\partial^2\theta}{\partial\xi^2} = -\mathrm{Re}[F(\xi,\tau)\exp(i\theta)]. \tag{14}$$

Equations (13) and (14) should be supplemented by conditions for electron phases in the plane of entry to the interaction space and the initial conditions for the field:

$$\theta(0) = \theta_0, \qquad \left.\frac{\mathrm{d}\theta}{\mathrm{d}\xi}\right|_{\xi=0} = -B, \qquad \theta_0 \in [0, 2\pi], \tag{15}$$

$$F(\xi, \tau = 0) = F_0(\xi). \tag{16}$$

Along with conditions (15) and (16), the boundary conditions for the field $F(\xi,\tau)$ at the ends of the interaction space are also required for complete formulation of the boundary-value problem. These will be conditions written below. The presented equations describe the processes near the low- or high-frequency edge of the transmission band depending on the chosen sign in excitation equation (13).

We note that when deriving equation of motion (14), one more approximation was used implicitly. Since we consider wave packets in which the synchronous components have wave numbers close to β_0, the group velocity of an electromagnetic wave along the system is small, and the field distribution $F(\xi,\tau)$ can be assumed almost constant during the time of transit of particles through the system. Hence, the time derivative is absent in Eq. (14).

The dimensionless variables and parameters are presented in Table 1. Table 1 also includes I_0, the total current of the electron beam, and V_0, the accelerating voltage of the electron beam. It is convenient to use the parameters B, Ω, and I for numerical calculations and the parameters Bl, Ωl^2, and l for analysis of the results, since the first two parameters in such a form are independent of the electron-beam current.

3. BOUNDARY CONDITIONS FOR ELECTRON MICROWAVE DEVICES OPERATED NEAR THE CUTOFF FREQUENCY

A significant feature of the theory describing a device operated near the cutoff frequency of an electrodynamic structure is adequate formulation of the boundary conditions responsible for the reflection of waves from the ends of a slow-wave system. Unlike the conventional TWT theory, which describes the field in terms of waves propagating in the positive and negative directions and converting into each other due to system inhomogeneities, the total field in our equations cannot be divided into such waves. Description of the reflection processes using reflection coefficients is meaningless near the cutoff. This is still more important since we want to describe not only propagating waves, but also the waves (with imaginary wavenumbers) outside the frequency band, for which the conventional notion of a reflection coefficient is absent.

Nevertheless, if reflection coefficients are used for the formulation of boundary conditions, then the following obstacle can be encountered. Let a small irregularity (see insert in Fig. 4) exist in a certain regular structure having a cutoff frequency (it does not matter whether this structure is homogeneous or periodic).

Generally, it can be shown that the coefficient of reflection from this irregularity behaves as is shown in Fig. 4. This magnitude of this reflection is exactly unity at the cutoff frequency ω_c and has the root singularity $\Gamma(\omega) = -1 + \mathcal{C}\sqrt{\omega - \omega_c}$, where $\mathcal{C}$ is a certain constant, at this point. Thus, the reflection coefficient is a nonanalytical function of frequency near the cutoff and, therefore, is strongly varied even with the small variation in frequency.

In order to understand what can be used instead of the reflection coefficient, consider the following situation [5]. Let a wave with frequency Ω be incident from the left onto the irregularity and be reflected from it. Assuming the time-harmonic dependence in the form $\exp(i\Omega\tau)$, we obtain for the wave a stationary equation in which the squared wavenumber is equal to $\pm\Omega$ for the low- and high-frequency cutoff, respectively:

$$\frac{\mathrm{d}^2 F}{\mathrm{d}\xi^2} + k^2 F = 0, \qquad k(\Omega) = \sqrt{\pm\Omega}. \tag{17}$$

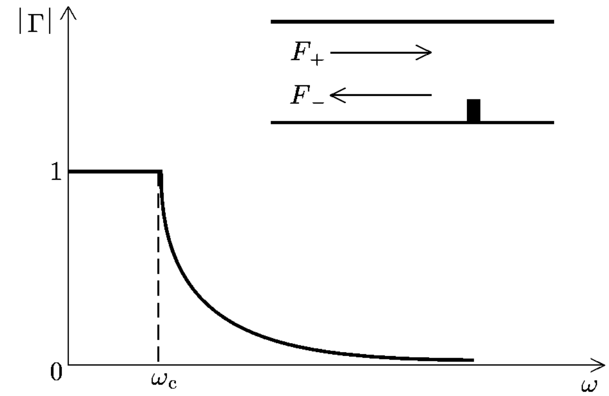

Fig. 4. Qualitative view of the dependence $|\Gamma(\omega)|$ for a wave reflected from an irregularity in a smooth waveguide.

Let us represent the solution in the form of a sum of two waves with amplitudes F_+ and F_-:

$$F(\xi) = F_+ \exp[-ik(\Omega)\xi] + F_- \exp[ik(\Omega)\xi]. \tag{18}$$

Differentiating Eq. (18) and assuming that the amplitudes of the waves incident on the irregularity and reflected from it are related in the plane $\xi = 0$ by the reflection coefficient, $F_+(0) = \Gamma(\Omega)F_-(0)$, we obtain an equation relating the derivative of the total field and the field itself,

$$[F'(\xi) + i\alpha(\Omega)F(\xi)]_{\xi=0} = 0, \tag{19}$$

in which the function $\alpha(\Omega)$ is determined by the expression

$$\alpha(\Omega) = k(\Omega)\frac{1 - \Gamma(\Omega)}{1 + \Gamma(\Omega)}\,. \tag{20}$$

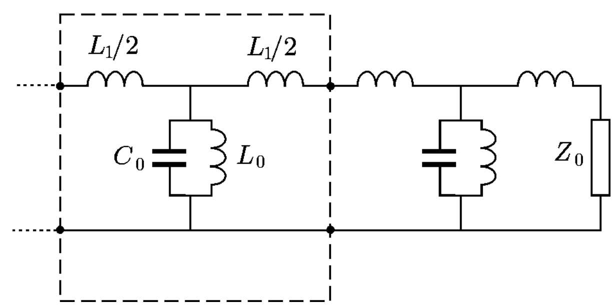

Fig. 5. Equivalent scheme of a simple model of a periodic structure based on coupled cavities. The dashed line shows one cell of the system.

Despite the fact that $k(\Omega)$ and $\Gamma(\Omega)$ have singularities, $\alpha(\Omega)$ is an analytical function of frequency within the transmission band and can be continued beyond the transmission band. Equation (19) represent the desired boundary condition for the field.

As an example, we consider a simple model of a periodic structure in the form of a chain of LC circuits coupled by inductances (Fig. 5). The irregularity in the system is modeled using the impedance Z_0 equal to the wave impedance of the energy-output line. Fairly simple calculations yield the expressions (in terms of dimensionless variables)

$$\Gamma(\omega) = -1 + \frac{\sqrt{2}\,Z_0\omega_0^{1/2}}{\omega\sqrt{L_1/C_0}}\sqrt{\omega - \omega_0} + \ldots\,, \qquad \alpha(\omega) = \frac{\omega L_1}{Z_0 d}\left[1 - \frac{2L_1C_0}{\sqrt{L_0C_0}}(\omega - \omega_0) + \ldots\right] \tag{21}$$

for the reflection coefficient and the function $\alpha(\Omega)$. Here, $\omega_0 = 1/\sqrt{L_0C_0}$, L_1/d is the inductance per unit length, and d is the typical size of a cell. It is seen that $\alpha(\omega)$ is indeed an analytical function of the frequency, although $\Gamma(\omega)$ has a root singularity. Since the function $\alpha(\omega)$ is analytical, it can be assumed constant, i. e., $\alpha(\omega) \approx \alpha(\omega_0)$, in a small frequency range near the cutoff frequency, and we will use this assumption in what follows.

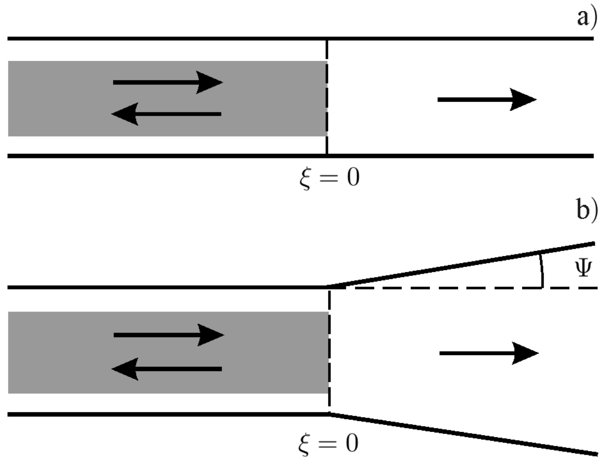

Fig. 6. The models used for the description of energy output in gyro-devices: perfect matching in the cross section $\xi = 0$ [15, 16] (*a*) and the waveguide loaded by a horn with a small opening angle [23] (*b*).

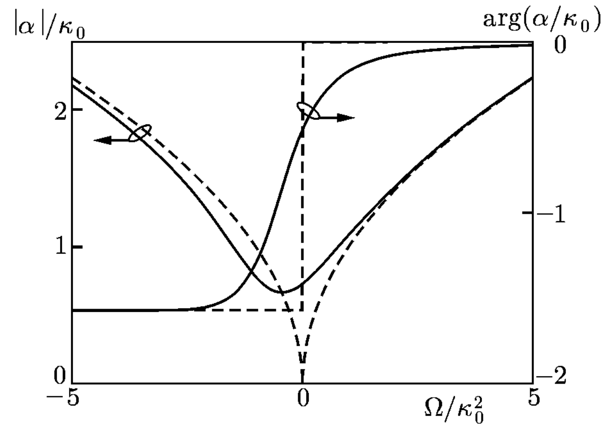

Fig. 7. Function $\alpha(\Omega)$ for the systems with diffraction energy output. The dashed line corresponds to the case of perfect matching, and the solid lines, to the case where the waveguide is loaded by a horn with a small opening angle.

It appears that for a number of devices, specifying the energy-output device permits one to obtain the function $\alpha(\Omega)$ in explicit form. There are several types of boundary conditions for which this can be done. We briefly consider two of them. Historically, perfect-matching conditions [15] were the first form of boundary conditions used for the description of reflections in relativistic devices with nonfixed field structure. These conditions were formulated for a gyrotron with nonfixed field structure, in which the electrodynamic structure represents a smooth waveguide with radius slowly varying along the longitudinal axis. The model used in [15] for the formulation of boundary conditions is shown in Fig. 6*a*. It is assumed that the region of field–beam interaction is located at $\xi < 0$ and that this region can be nonuniform. The waveguide is uniform on the right of the point $\xi = 0$, so that the wave reflection is absent in this region. Then, only the waves escaping from the interaction region must exist for $\xi > 0$. Assuming that the signal spectrum in such a system is narrow, it is easy to obtain boundary conditions in form (19), in which the function $\alpha(\Omega)$ is defined as follows:

$$\alpha(\Omega) = \sqrt{\Omega}\,. \tag{22}$$

If the signal frequency is not too close to the cutoff, then the assumption that reflections are absent is valid. However, if the signal spectrum is very close to the cutoff frequency, then this approximation ceases to be physically reasonable. It suffices to say that exactly at the cutoff frequency, as was mentioned above, an infinitesimal inhomogeneity on the right of the output cross section leads to the appearance of finite reflections. Hence, for any actual system, the signal components with frequencies close to cutoff will undergo strong reflections. Since the regimes of generation or amplification of oscillations near the cutoff in the mentioned systems is of particular interest, it seems natural to consider a more realistic system in which the interaction space ends with a horn used for energy output (Fig. 6*b*). In this case, the boundary condition retains form (19), while the function $\alpha(\Omega)$ is equal to [23]

$$\alpha(\Omega) = \kappa_0 \exp(5i\pi/6)\frac{\mathrm{Ai}'(\exp(i\pi/3)\Omega/\kappa_0^2)}{\mathrm{Ai}(\exp(i\pi/3)\Omega/\kappa_0^2)}\,, \qquad \kappa_0 = \frac{(2\Psi\nu_{nm}^2)^{1/3}}{R_0}\,, \tag{23}$$

where $\mathrm{Ai}(x)$ is an Airy function, ν_{nm} are the roots of a Bessel-function derivative, $J_n'(\nu_{nm}) = 0$, and the parameter κ_0 is expressed in terms of geometric parameters of the system, i. e., the opening angle Ψ of the horn and the waveguide radius R_0. The modulus and argument of the function $\alpha(\Omega)$ are plotted by the solid lines in Fig. 7. The same quantities for the function $\alpha(\Omega)$ given by Eq. (22) are shown by the dashed lines.

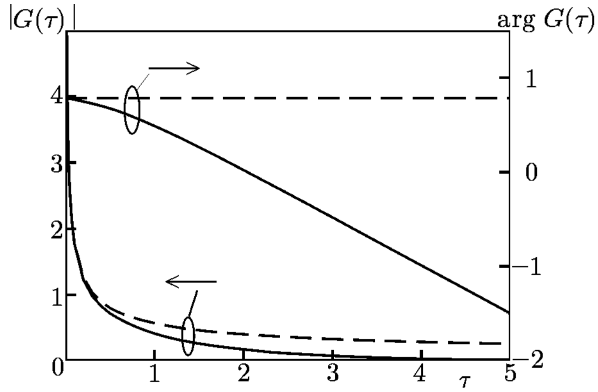

Fig. 8. Function $G(\tau)$ for nonstationary boundary conditions (24). The dashed lines correspond to the case of perfect matching, and the solid lines, the case where the waveguide is loaded by a horn with a small opening angle.

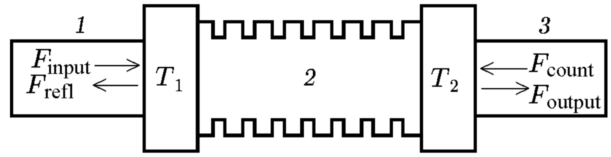

Fig. 9. The model of a coupled-cavity TWT used for the analysis: *1*, the input waveguide, *2*, the interaction space, *3*, the output waveguide, and T_1 and T_2, the matching devices.

The obtained boundary conditions are valid for one spectral component. Obtaining boundary conditions in the temporal representation requires using the inverse Fourier transform for Eq. (19). Then the nonstationary boundary condition takes the form

$$F(0,\tau) - i\int\limits_0^\tau G(\tau-\tau')\frac{\partial F(0,\tau-\tau')}{\partial\xi}\,\mathrm{d}\tau' = 0, \tag{24}$$

where

$$G(\tau) = \exp(i\pi/4)/\sqrt{\pi\tau} \tag{25}$$

for the case of perfect matching [16], i. e., where the function $\alpha(\Omega)$ is given by Eq. (22), and

$$G(\tau) = \exp(i\pi/3)\sum_{n=1}^{\infty}\frac{\exp(-a_n'\exp(i\pi/6)\tau)}{a_n'} \tag{26}$$

if a horn is used as the output device [23] (the function $\alpha(\Omega)$ is given by Eq. (23)). In Eq. (26), a_n' are the absolute values of the arguments for which the Airy-function derivative becomes zero. A method for efficient calculation of the sum in Eq. (26) is presented in [23]. The form of the function $G(\tau)$ for both cases is shown in Fig. 8 (the solid lines correspond to Eq. (26) and the dashed lines, to Eq. (25)).

It should be mentioned that the obtained nonstationary boundary conditions are nonlocal in time, i. e., the field in the output plane at the time instant τ depends on the field values at all the previous time instants. The presence of such nonlocal coupling is explained by the strong dispersion of the waves propagating in the output device at near-cutoff frequencies.

Returning to boundary conditions for description of the processes in a coupled-cavity TWT, we note that the periodic structure in such a device is connected to the input and output sections via the matching devices T_1 and T_2, as is shown in Fig. 9, and the parameters are chosen such that to minimize dispersion in the input and output sections for the operating frequency range. In this case, the function $\alpha(\Omega)$ in the boundary condition is slowly varied in the operating frequency range, and can be assumed constant with good accuracy [5]. This considerably simplifies modeling of nonstationary processes since in this approximation, the boundary conditions in the nonstationary case have the same form as in the stationary theory.

It can be assumed that in the most general formulation, the signals are fed into the system from both the gun and the collector ends. We designate their amplitudes by $F_{\text{input}}(\tau)$ and $F_{\text{count}}(\tau)$. Reflections of these waves from the ends of the system as well as output of energy from the interaction space in the feed sections result in the formation of waves traveling off the periodic structure. We designate their amplitudes by $F_{\text{refl}}(\tau)$ and $F_{\text{output}}(\tau)$ (see Fig. 9). Then the boundary conditions describing these processes at both ends of the interaction space take the form [5]

$$\left[\frac{\partial F(\xi,\tau)}{\partial \xi} \pm i\alpha_1 F(\xi,\tau)\right]_{\xi=0} = F_{\text{input}}(\tau), \tag{27a}$$

$$\left[\frac{\partial F(\xi,\tau)}{\partial \xi} \mp i\alpha_1 F(\xi,\tau)\right]_{\xi=0} = F_{\text{refl}}(\tau), \tag{27b}$$

$$\left[\frac{\partial F(\xi,\tau)}{\partial \xi} \mp i\alpha_2 F(\xi,\tau)\right]_{\xi=l} = F_{\text{count}}(\tau), \tag{27c}$$

$$\left[\frac{\partial F(\xi,\tau)}{\partial \xi} \pm i\alpha_2 F(\xi,\tau)\right]_{\xi=l} = F_{\text{output}}(\tau). \tag{27d}$$

In these formulas, the choice of the sign is determined by the cutoff type: the upper sign corresponds to the high-frequency, and the lower sign, the low-frequency edge of the transmission band. Rigorously speaking, only Eqs. (27a) and (27c) are the boundary conditions in Eq. (27), while the remaining Eqs. (27b) and (27d) determine the signals $F_{\text{refl}}(\tau)$ and $F_{\text{output}}(\tau)$ escaping from the system in the input and output sections.

Hereafter, to reduce the number of parameters, we consider various operation regimes of the device assuming that the feed sections and the matching transformers are identical and the system is completely matched at a certain point of the transmission band. Then the dimensionless parameters $\alpha_1 l$ and $\alpha_2 l$ are equal to each other and are approximately determined by the formula $\alpha_1 l = \alpha_2 l = \alpha l \approx |\beta_{\text{match}} - \beta_0|\, L$, where β_{match} is the wavenumber of the "cold" wavenumber of the system at the matching point. According to estimates, the realistic values of the parameter αl for a coupled-cavity TWT amount to about $5-50$ [5, 6].

Equations (13)–(16) together with boundary conditions (27a) and (27c) completely determine the dynamics of the system in all possible operation regimes.

4. LINEAR THEORY OF A COUPLED-CAVITY TWT: AMPLIFICATION AND PARASITIC SELF-EXCITATION

For considering stationary linear operation regimes of a coupled-cavity TWT, we assume that all quantities have the time-harmonic dependence $\exp(i\Omega\tau)$. Then, transforming the equations of motion of electrons to the equation for the dimensionless current amplitude $I(\xi)$, we obtain the following equations describing the operation of the device [6, 7, 12]:

$$\mp\frac{\mathrm{d}^2 F(\xi)}{\mathrm{d}\xi^2} + \Omega F(\xi) = iI(\xi), \qquad \left(\frac{\mathrm{d}}{\mathrm{d}\xi} - iB\right)^2 I(\xi) = iF(\xi). \tag{28}$$

These equations are supplemented by the boundary conditions for the current at $\xi = 0$,

$$I(0) = 0, \qquad I'(0) = 0, \tag{29}$$

as well as by the boundary conditions for the field, which follow from Eqs. (27a) and (27c), putting $F_{\text{count}} = 0$ and $F_{\text{input}}(\tau) = \bar{F}_{\text{input}} \exp(i\Omega\tau)$ and omitting the common exponential factor. We find the complex amplitude $\bar{F}_{\text{output}}$ of the output signal from Eq. (27d) transformed in the same manner.

The dependences of the gain of a coupled-cavity TWT in the linear regime on the mismatch parameter B, calculated for different frequencies, are shown in Figs. 10 and 11 for the high- and low-frequency edges of the transmission band, respectively. The results obtained using the discrete approach [6] are shown by dots in these figures for comparison. It is seen that the coincidence of the results calculated near the

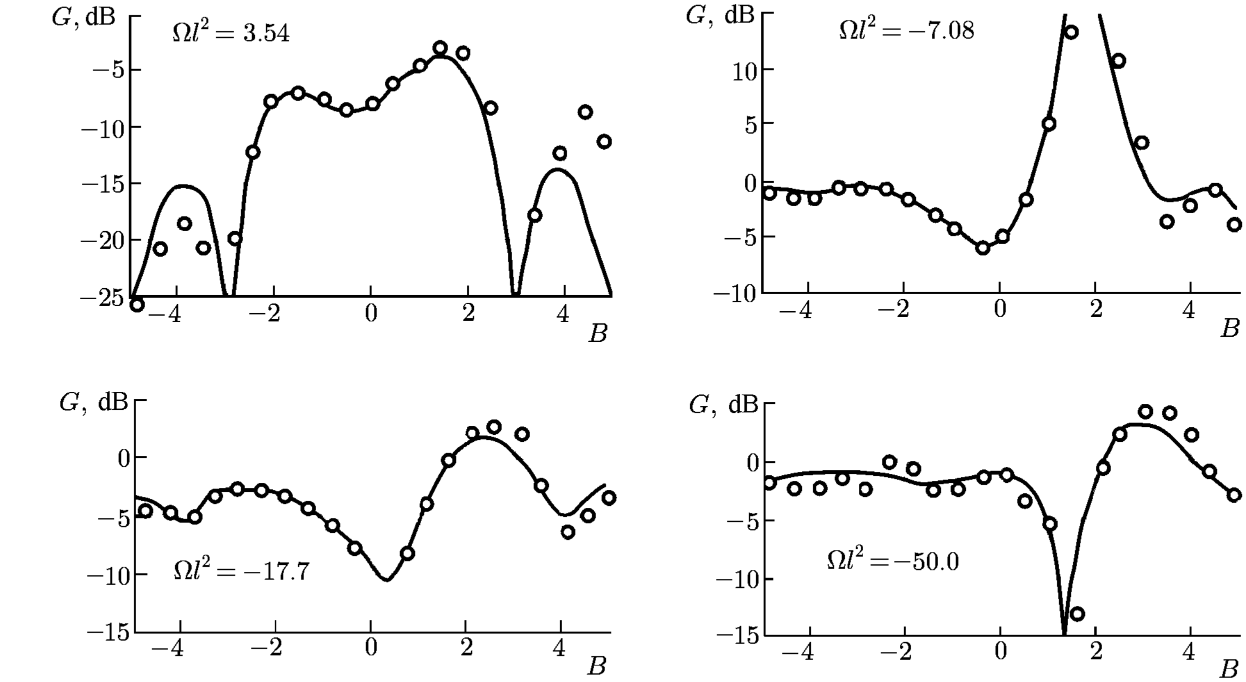

Fig. 10. Gain of a coupled-cavity TWT in the linear regime in the case of interaction near the high-frequency cutoff. The dots correspond to a calculation in terms of the discrete theory [6].

high-frequency cutoff is fairly good. The dependences for a different number N of cells in the slow-wave system for the low-frequency edge are shown in Fig. 11. A certain difference in the results disappears as N increases.

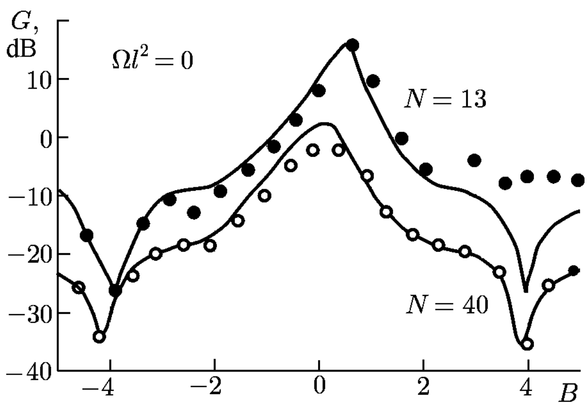

Fig. 11. Gain of a coupled-cavity TWT in the linear regime in the case of interaction near the low-frequency cutoff. The dots correspond to a calculation in terms of the discrete theory.

One of the important problems in the study of operation regimes of a TWT is analysis of the parasitic self-excitation at frequencies near cutoff [7, 9]. The starting conditions of parasitic generation can be found by joint solution of Eqs. (28) of the linear theory, conditions (29) for the current, and boundary conditions (27a) and (27c), in which one should put $F_{\text{input}} = 0$ and $F_{\text{count}} = 0$. The requirement that a nontrivial solution of this system of equations should exist leads to the starting conditions of generation:

$$\sum_{i=1}^{4} \frac{(k_i \pm \alpha_1)(k_i \pm \alpha_2)\exp(-ik_i l)}{k_i + (k_i \pm \Omega)/(k_i + B)} = 0, \qquad (30)$$

where k_i are the roots of the dispersion equation

$$(k^2 \pm \Omega)(k + B)^2 - 1 = 0. \qquad (31)$$

If the boundary-condition parameters $\alpha_1 = \alpha_2 = \alpha$ and the mismatch parameter are fixed, then complex equation (30) permits one to find the real quantities l and Ω, i. e., the dimensionless starting length and the self-excitation frequency. We represent the calculation results in the form of the dependences $l(Bl)$ and $\sqrt{|\Omega|}\, l(Bl)$.

Consider at first the self-excitation near the high-frequency cutoff. The results of numerical calculation of the starting parameters are presented in Fig. 12 for different values of the parameter αl. In these diagrams, an increase in the parameter Bl corresponds to an increase in the accelerating voltage of the

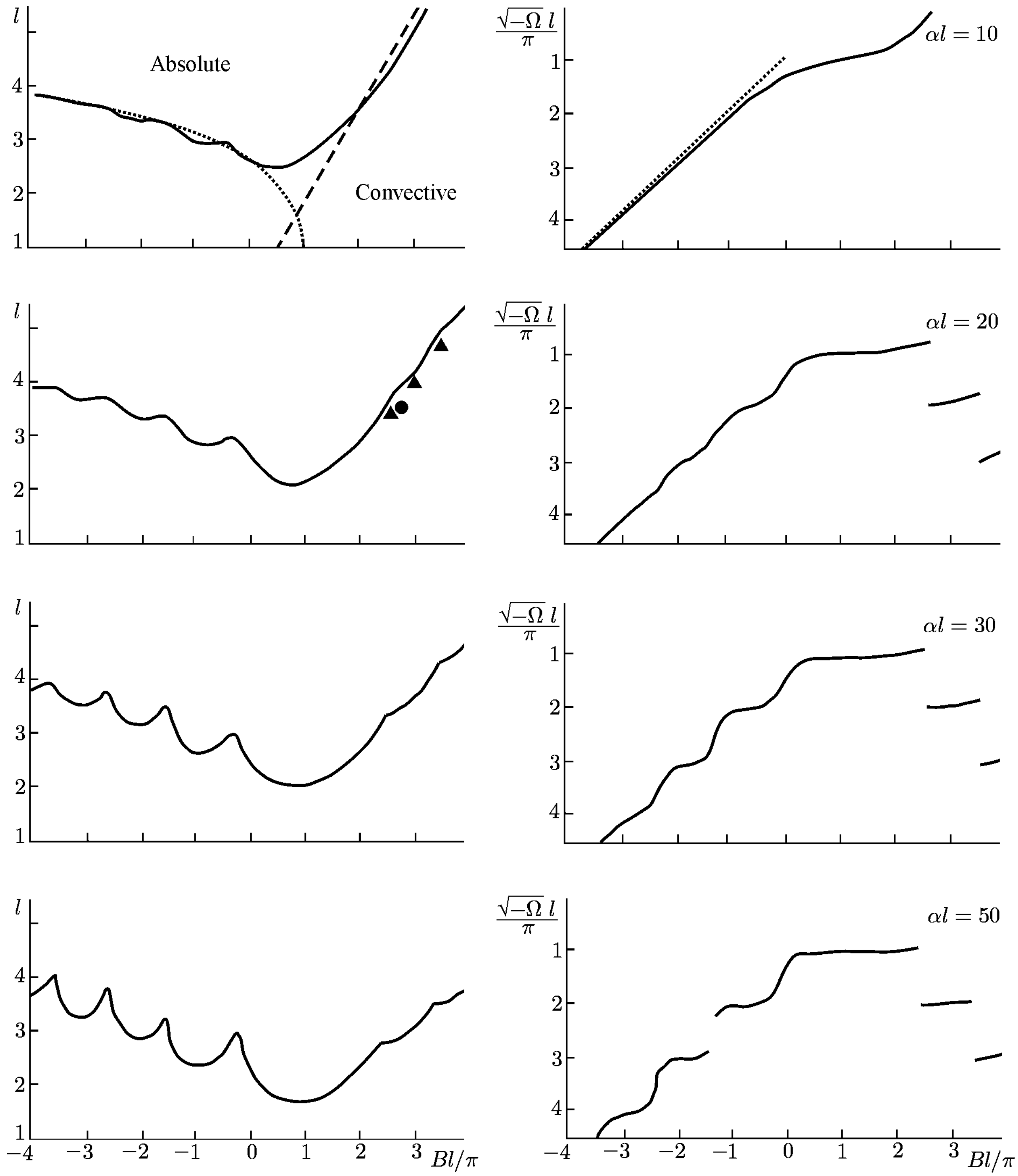

Fig. 12. Starting conditions of self-excitation of a TWT near the high-frequency cutoff. In the upper plots, the dashed line shows the starting conditions for a BWT and the dotted line separates the domains in which the absolute and convective instabilities in a system with infinite length are realized.

electron beam and a transition from the regime of predominant interaction with a backward wave to the regime of predominant interaction with a forward wave.

Two mechanisms responsible for the excitation of a TWT near the high-frequency cutoff can be mentioned. The first mechanism is realized for large values of αl and is related to the excitation of resonant modes. By definition, the quantity αl determines the properties of a "cold" system and the intensity of the electromagnetic field radiated from it. For large values of this parameter, the resonance properties of

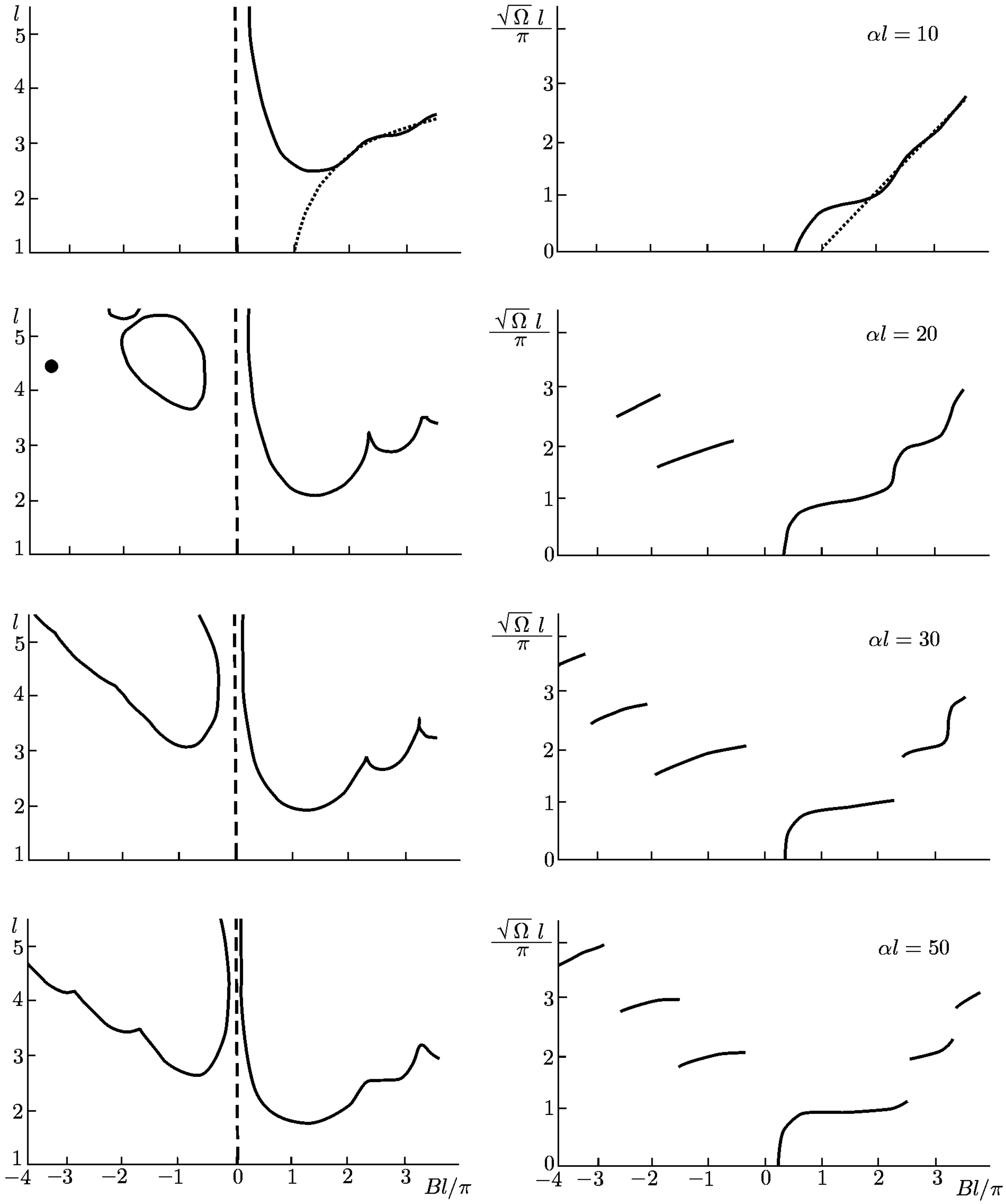

Fig. 13. Starting conditions of self-excitation of a TWT near the low-frequency cutoff. The designations for the lines are the same as in Fig. 12.

the system have an effect, and the electron beam efficiently interacts with the forward wave component (resonant mode) if $n\pi < Bl < n\pi + 2\pi$ or with the backward wave component if $n\pi - 2\pi < Bl < n\pi$. If one of these conditions is satisfied, then self-excitation of the nth mode will occur for the corresponding current, and the starting lines $\sqrt{|\Omega|}\, l(Bl)$, determining the starting frequencies, will resemble steps with frequency varied only slightly with the variation in the electron-beam velocity.

With decrease in the parameter αl, the system loses its resonance properties, and the described self-excitation picture changes. In the case of small αl, the mechanism of excitation of oscillations in the system is not related to reflections of an electromagnetic wave from the ends of a slow-wave system, and the mechanism stipulated by the presence of distributed feedback due to interaction with a backward wave is realized in this case. In the region of the negative values of Bl, the self-excitation occurs in the same way as in a conventional TWT, as is clearly seen in Fig. 12 for $\alpha l = 10$, where the dashed line corresponds to the starting conditions of BWT self-excitation. In the case of synchronism between the electron beam and the forward wave ($Bl > 0$), the self-excitation occurs due to the specific mechanism related to the possibility of existence of the absolute instability in the system near the high-frequency cutoff even if synchronism with predominantly forward waves takes place [8]. The dashed line in the same figure separates the domains in the parameter plane (Bl, l) in which the absolute and convective instabilities in an infinitely long system described by dispersion equation (31) are realized.

It is interesting to note that the minimum starting current corresponds to such an accelerating voltage of the electron beam for which the synchronism point is still located on the forward branch of the dispersion curve. This fact explains the increased hazard of self-excitation of a coupled-cavity TWT exactly near the high-frequency edge of the transmission band [7].

For the case of interaction near the low-frequency cutoff, the results of calculation of the starting conditions are shown in Fig. 13. Now, an increase in voltage (or in the parameter Bl) leads to a transition from interaction between the electron beam and the forward branch of the dispersion curve of the cold system to interaction with the backward branch. On the whole, the starting characteristics of the parasitic generation remain qualitatively the same as for the case of a high-frequency cutoff. However, in the case of small reflections from the ends of a slow-wave system, self-excitation on the forward branch now corresponds to very large starting currents. This is related to the fact that the boundary between the absolute and convective instabilities now corresponds to the value $Bl = 0$ (dashed line in Fig. 13). Hence, if the electron beam is in synchronism with the forward wave, then reflections of a signal from the ends of the system are the only reason for self-excitation. It is interesting to note that in the case of exact synchronism between the electron beam and the field at the cutoff frequency, the starting current turns out to be equal to the infinity. The minimum of the starting current lies in the region of synchronism with backward waves. As the level of reflections from the ends of the system increases gradually, the resonance mechanism of self-excitation also begins to be play a role (see Fig. 13 for $\alpha l = 30; 50$).

5. NONSTATIONARY EFFECTS

To study the broader range of problems related to interaction between an electron beam and an electromagnetic field, one should use the approach based on nonstationary nonlinear equations describing this interaction [4, 13, 14]. The main advantage of the nonstationary approach is that it allows not to make *a priori* assumptions on the nature of the stationary regime of oscillations. This regime is found in a natural way as a result of modeling of the temporal behavior of the system, and the problem of stability of the found regime is also solved correspondingly. In such complex distributed dynamic systems as "electron beam — electromagnetic wave," various oscillation regimes, including stationary, periodic, and chaotic, are possible, and some nontrivial effects, whose prediction and analysis are possible only within the framework of the nonstationary approach, can also occur there. Several such effects are considered below.

To study the nonstationary processes, we performed numerical simulation of Eqs. (13) and (14), supplemented with initial conditions (15) and (16). The boundary condition for the field at the right-hand end of the interaction space was specified by Eq. (27c). It was assumed in this equation that $F_{\text{count}} = 0$, and the boundary condition at the gun end of the tube was determined by the type of the problem being solved.

As the first effect, we consider the self-excitation of a coupled-cavity TWT, initiated by an amplified signal. We assume that a monochromatic signal is fed at the tube input. In this case, the boundary condition for $\xi = 0$ should be taken in form (27a) by putting $F_{\text{input}}(\tau) = F^0_{\text{input}} \exp(i\Omega\tau)$ for $\tau > 0$, where Ω is the frequency of the input signal.

Consider at first the process of onset of the stationary regime of amplification where the interaction occurs near the low-frequency edge of the transmission band. Figure 14 shows the temporal dependences of the output-signal amplitude for $\Omega l^2 = 121$, $Bl = -3.5\pi$, $l = 4.5$, and $\alpha_1 l = \alpha_2 l = 20$. The curves in this figure correspond to different values of the initial amplitude of the input signal. It is seen that all the transient processes at the low-frequency cutoff lead to the onset of stationary oscillations with constant amplitude and frequency equal to the frequency of the signal fed to the input, even if the input-signal amplitude is fairly large. Taking into account nonlinear effects at the low-frequency edge of the transmission band leads only to a decrease in the gain with increase in the input-signal amplitude.

A different process can be observed at the high-frequency edge of the transmission band. Let, e. g., the parameters $Bl = 2.8\pi$, $l = 3.5$, and $\Omega l^2 = -30.6$ be chosen. In this case, if the input-signal amplitude is relatively small ($F^0_{\text{input}} = 2.0$), then stationary regimes are settled after the transient process (Fig. 15*a*). However, if a fairly powerful signal with $F^0_{\text{input}} = 4.0$ is supplied to the input, then signal-amplitude oscillations not decaying with time are observed.

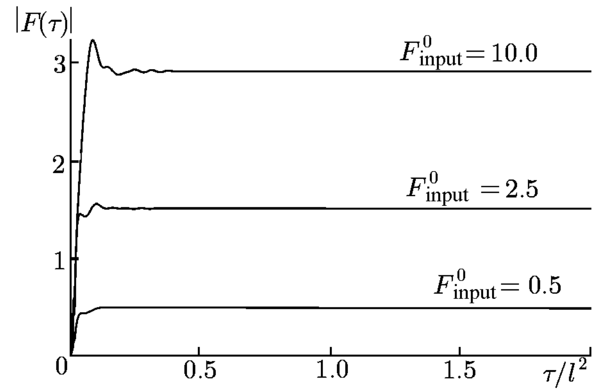

Fig. 14. Onset of the stationary regime of amplification in the case of interaction near the low-frequency cutoff. The curves correspond to different values of the input-signal power.

Figure 15 also shows the input-signal spectra in both cases. For a small input power, the spectrum comprises a single line whose frequency is equal to the input-signal frequency. In the second case, the spectrum is discrete and contains a component at the frequency of the amplified signal and the main parasitic component having the frequency $\Omega l^2 \approx -9.9$ close to the eigenfrequency of the first resonant mode of the "cold" system ($\Omega l^2 \approx -\pi^2$). The remaining lines in the spectrum represent various combinations of these frequencies.

The considerably different behavior of the system near the low- and high-frequency edges of the transmission band is related to the nonlinear effects of deceleration of the electron beam by the radiation field. The black circles in Figs. 12 and 13 show the points in the parameter plane (Bl, l) at which the simulation was performed. For the high-frequency cutoff, deceleration of the electron beam and a decrease in its average velocity lead to an efficient decrease in the parameter Bl. In this case, the operating point in Fig. 12 is shifted to the left and enters the self-excitation area. Near the low-frequency cutoff, on the contrary, a decrease in the parameter Bl owing to the nonlinear deceleration shifts the operating point off the self-excitation area (see Fig. 13), and, therefore, the parasitic oscillation does not occur.

Hard excitation of oscillations is another nonlinear effect that can be observed in a coupled-cavity TWT during interaction near the cutoff. As an example, we consider interaction near the high-frequency cutoff. The triangles in Fig. 12 show the points at which the onset of oscillations in the system was simulated in the absence of the input signal. The initial distribution of the field was assigned in the form of the first resonance mode $F(\xi, 0) = F_0 \sin(\pi\xi/l)$, and the calculations were performed for different values of the initial amplitude F_0. The obtained results are given in Fig. 16 in the form of temporal dependences of the amplitudes of the signals radiated from the system into the output section (solid line) and the input section (dashed line). Figure 16*a* corresponds to the parameters $Bl = 2.5$ and $l = 3.4$, Fig. 16*b*, to the parameters $Bl = 3$ and $l = 4$, and Fig. 16*c*, to the parameters $Bl = 3.5$ and $l = 4.7$. The effect of hard excitation of oscillations was observed. In all three cases. For small amplitudes of the initial distribution of the field, oscillations completely decay with time. However, if the quantity F_0 exceeds a certain threshold value, then stationary oscillations are settled in the system as a result of the transient process. In this case, the field distribution along the interaction space and the oscillation frequency correspond to the first resonance mode of the "cold" system.

Hard excitation is also related to the fact that for a large signal amplitude, the nonlinear deceleration of the electron beam in the chosen parameter region in the plane (Bl, l) improves interaction between

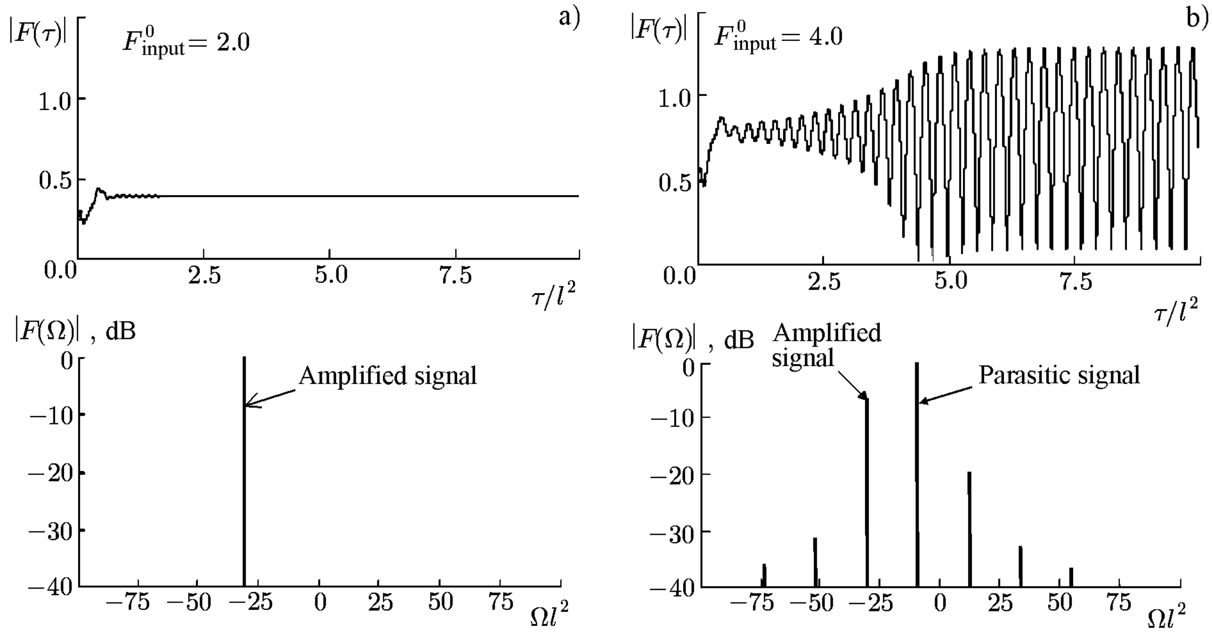

Fig. 15. The self-excitation initiated by a high-power input signal during interaction near the high-frequency cutoff. Onset of oscillations for relatively small (*a*) and large (*b*) input powers. The upper plots show the temporal dependences of the output-signal amplitude, and the lower plots, the output-signal spectra.

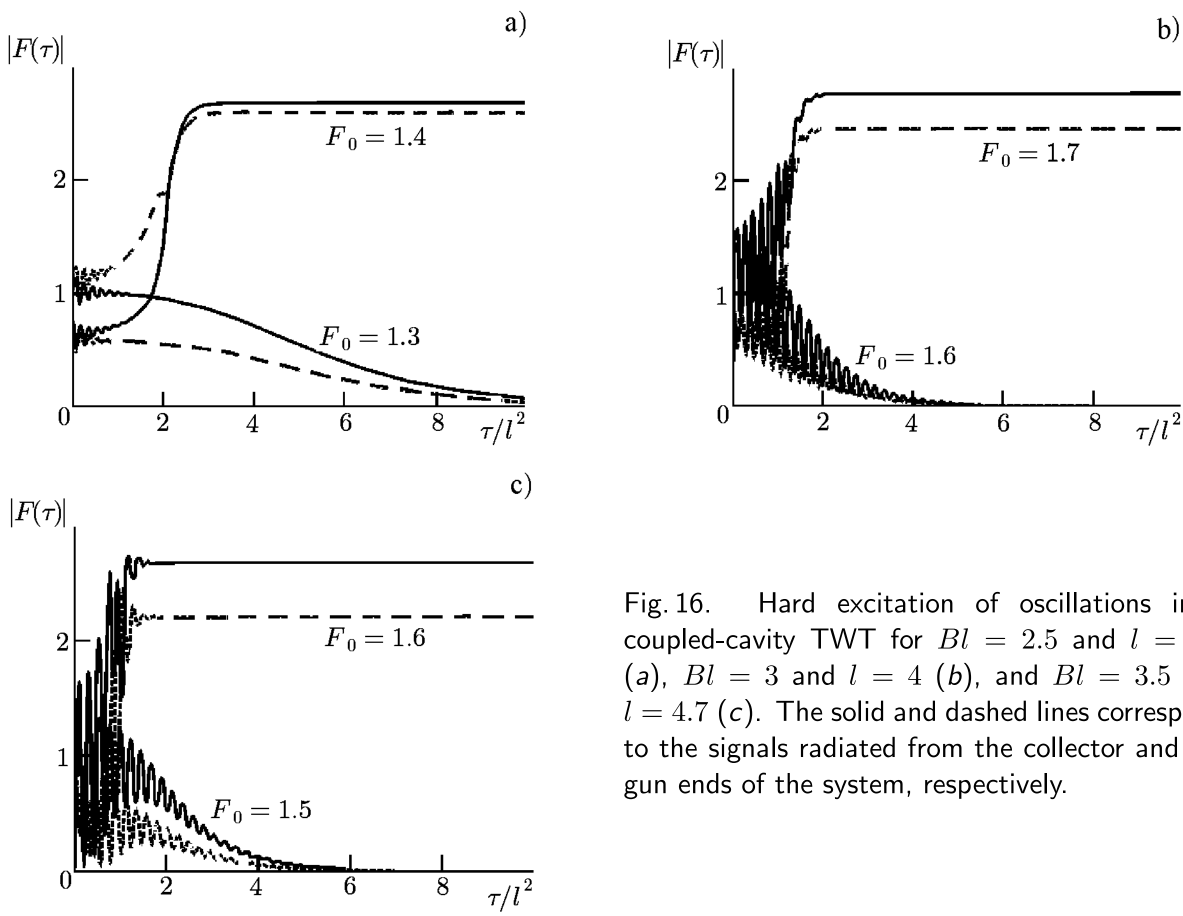

Fig. 16. Hard excitation of oscillations in a coupled-cavity TWT for $Bl = 2.5$ and $l = 3.4$ (*a*), $Bl = 3$ and $l = 4$ (*b*), and $Bl = 3.5$ and $l = 4.7$ (*c*). The solid and dashed lines correspond to the signals radiated from the collector and the gun ends of the system, respectively.

the electrons and the field of the first resonance mode. While this process is inefficient in the linear regime, the oscillations turn out to be self-sustained in the nonlinear regime, i. e., for a large signal amplitude.

Observation of the hysteresis phenomenon near the boundary of the oscillation domain also becomes possible owing to the possibility of hard excitation of oscillations in the system. When passing through this boundary, oscillations with finite amplitude will arise in the system, but if, by varying the parameters, the linear oscillation domain is reached, then these oscillations will exist till their quenching for a certain finite displacement from the oscillation-domain boundary.

6. CONCLUSIONS

Development of the wave theory of interaction between electron beams and electromagnetic waves near the edge of the transmission band is of fundamental interest for microwave electronics. Indeed, such a theory should bridge the obvious gap. While interaction separately with forward or backward waves was qualitatively understood and theoretically studied a long time ago, the problem of describing the intermediate situation where the synchronism region of an electron beam and oscillations in the electrodynamic structure is located near the cutoff has for a long time presented difficulties and, fundamentally, remained unsolved. At the same time, understanding of the features of the interaction near the cutoff is important for a variety of microwave electronic devices such as a coupled-cavity TWT, an orotron, a gyrotron, etc.

From the theoretical viewpoint, a study of devices operated at the cutoff is of particular interest since they combine in a nontrivial way the features typical of devices with forward waves and with counterpropagating waves as well as devices with localized cavity oscillations. The use of the nonstationary nonlinear theory for describing the dynamics of electron oscillators and amplifiers operated near the cutoff is especially important since in this case, the realized regime is specified immediately during numerical simulation of the onset of oscillations.

The series of papers included in the present overview developed the wave theory of interaction between an electron beam and the field of an electrodynamic structure near the cutoff, in which all fundamental difficulties were overcome. This theory is constructed with allowance for the specific features of the long-term interaction, is simple, and offers the minimum set of significant parameters. Moreover, this theory includes all the main effects realized near the cutoff of the transmission band and gives a qualitatively clear picture of these effects. All the variables and parameters used in the model do not have singularities or divergences and, therefore, are good for measurement and practical application. Obviously, the developed theory and the picture of phenomena based on it will help considerably with the development and optimization of microwave electron devices operated near the cutoff.

This work was supported by the Russian Foundation for Basic Research (project Nos. 03–02–16192 and 02–02–17317).

REFERENCES

1. L. V. Bulgakova, D. I. Trubetskov, V. L. Fisher, and V. N. Shevchik, in: *Lectures in O-Type Microwave Device Electronics* [in Russian], Saratov State Univ., Saratov (1974), p. 221.

2. V. A. Solntsev and A. V. Osin, in: *Lectures in Microwave Electronics amd Radiophysics. The 5th Winter Workshop of Engineers, Book 4* [in Russian], Saratov State Univ., Saratov (1981), p. 142.

3. S. V. Mukhin and V. A. Solntsev, in: *Lectures in Microwave Electronics and Radiophysics. The 7th Winter Workshop of Engineers, Book 1* [in Russian], Saratov State Univ. Press, Saratov (1986), p. 43.

4. A. P. Kuznetsov and S. P. Kuznetsov, *Radiophys. Quantum Electron.*, **27**, No. 12, 1099 (1984).

5. A. P. Kuznetsov, *Élektron. Tekh., Ser. 1, Élektron. SVCh*, No. 7(367), 3 (1984).

6. L. V. Bulgakova, M. V. Gavrilov, A. P. Kuznetsov, et al., *Élektron. Tekh., Ser. 1, Élektron. SVCh*, No. 6(378), 34 (1985).

7. A. P. Kuznetsov and A. G. Rozhnev, *Élektron. Tekh., Ser. 1, Élektron. SVCh*, No. 9(381), 3 (1985).

8. A. P. Kuznetsov, *Sov. Tech. Phys. Lett.*, **8**, No. 15, 408 (1982).

9. A. P. Kuznetsov, S. P. Kuznetsov, and A. G. Rozhnev, in: *Lectures in Microwave Electronics and Radiophysics. The 7th Winter Workshop of Engineers, Book 2* [in Russian], Saratov State Univ., Saratov (1986), p. 44.

10. L. V. Bulgakova and S. P. Kuznetsov, in: *Lectures in Microwave Electronics and Radiophysics. The 7th Winter Workshop of Engineers, Book 2* [in Russian], Saratov State Univ., Saratov (1986), p. 56.

11. A. P. Kuznetsov and A. G. Rozhnev, *Radiophys. Quantum Electron.*, **31**, No. 9, 793 (1988).

12. L. V. Bulgakova, A. P. Kuznetsov, S. P. Kuznetsov, and A. G. Rozhnev, *Élektron. Tekh., Ser. 1, Élektron. SVCh*, No. 3(407), p. 7 (1988).

13. L. V. Bulgakova and S. P. Kuznetsov, *Radiophys. Quantum Electron.*, **31**, No. 2, 155 (1988).

14. L. V. Bulgakova and S. P. Kuznetsov, *Radiophys. Quantum Electron.*, **31**, No. 5, 452 (1988).

15. V. L. Bratman, M. A. Moiseev, M. I. Petelin, and R. É. Érm, *Radiophys. Quantum Electron.*, **16**, No. 4, 474 (1973).

16. N. S. Ginzburg, N. A. Zavol'skii, G. S. Nusinovich, and A. S. Sergeev, *Radiophys. Quantum Electron.*, **29**, No. 1, 89 (1986).

17. V. A. Solntsev and N. P. Kravchenko, *Radiotekh. Élektron.*, **23**, No. 5, 1103 (1978).

18. A. V. Osin and V. A. Solntsev, *Radiotekh. Élektron.*, **24**, No. 7, 1380 (1979).

19. N. P. Kravchenko and V. A. Solntsev, *Radiotekh. Élektron.*, **25**, No. 3, 601 (1980).

20. A. V. Osin and V. A. Solntsev, *Radiotekh. Élektron.*, **27**, No. 11, 2207 (1982).

21. A. V. Osin and V. A. Solntsev, *Radiotekh. Élektron.*, **27**, No, 12, 2435 (1982).

22. S. P. Kuznetsov, *Radiotekh. Élektron.*, **25**, No 2, 419 (1980).

23. A. G. Rozhnev, *J. Commun. Techn. Electron. Suppl.*, **45**, No. 1, 95 (2000).